Journal of Catalysis **207,** 266–273 (2002)
doi:10.1006/jcat.2002.3524, available online at http://www.idealibrary.com on IDEAL®

Synthesis, Characterization, and Hydrodesulfurization Properties of Silica-Supported Molybdenum Phosphide Catalysts

Diana C. Phillips, Stephanie J. Sawhill, Randy Self, and Mark E. Bussell[1]

Department of Chemistry, MS-9150, Western Washington University, Bellingham, Washington 98225

Received July 26, 2001; revised January 15, 2002; accepted January 15, 2002

Silica-supported molybdenum phosphide (MoP/SiO_2) catalysts have been prepared and characterized by X-ray diffraction (XRD), pulsed chemisorption (CO and O_2), scanning and transmission electron microscopy (SEM and TEM, respectively), and X-ray photoelectron spectroscopy (XPS). XRD and TEM analysis of MoP/SiO_2 catalysts confirmed the presence of MoP crystallites dispersed on the surface of the silica support, while SEM energy dispersive X-ray microanalysis indicated the bulk composition of the supported MoP particles to be 12.7 atom% Mo and 14.1 atom% P. XPS analysis of a passivated 25 wt% MoP/SiO_2 catalyst indicated the presence of two kinds of Mo species as well as phosphide and phosphate species at the catalyst surface. Thiophene hydrodesulfurization (HDS) activities were measured for 15 and 25 wt% MoP/SiO_2 catalysts, and for a sulfided Mo/SiO_2 catalyst with a Mo loading similar to that of the lower loading MoP catalyst. The 15 wt% MoP/SiO_2 catalyst, when pretreated only by degassing in flowing He, was nearly four times more active than the sulfided Mo/SiO_2 catalyst after 150 h on-stream. Following an initial decline in HDS activity during the first 3 h of measurement, the MoP/SiO_2 catalyst displayed an unusual trend of HDS activity that increased monotonically as a function of time on-stream.

INTRODUCTION

Considerable effort has been devoted to optimizing Mo sulfide-based hydrodesulfurization (HDS) catalysts and nearly a twofold increase in HDS activity has been achieved over the last 30 years (1). Environmental legislation recently passed or proposed in many countries will dramatically lower allowable sulfur levels in transportation fuels. When the requirement for lower sulfur levels in fuels is coupled with the need to process lower quality petroleum feedstocks in coming years, the general consensus is that incremental improvements in the current sulfide-based HDS catalysts will not be sufficient.

One approach to the development of new HDS catalysts is to investigate how main group elements other than sulfur modify the catalytic properties of molybdenum. Studies in a number of laboratories over the past few years have shown oxide-supported molybenum carbide (β-Mo_2C) (2–4) and nitride (γ-Mo_2N) (3–7) to be more active HDS catalysts than conventional sulfided molybdenum catalysts. More recently, a few studies have appeared which show that molybdenum phosphide (MoP) has high catalytic activity for hydrodenitrogenation (HDN) (8–10) and HDS (8, 10). In the current study, we report the successful synthesis of silica-supported molybdenum phosphide (MoP/SiO_2) and describe its characterization and HDS catalytic properties.

[1] To whom correspondence should be addressed. Fax: 360-650-2826. E-mail: Mark.Bussell@wwu.edu.

EXPERIMENTAL METHODS

Catalyst Preparation

MoP. Unsupported molybdenum phosphide was prepared using a procedure reported elsewhere (8, 9). A mixture of 4.0 g (3.24 mmol) of ammonium heptamolybdate $(NH_4)_6Mo_7O_{24} \cdot 4H_2O$ (Alfa–Aesar) and 3.0 g (22.72 mmol) of diammonium hydrogen phosphate $(NH_4)_2HPO_4$ (Alfa–Aesar) was dissolved in 15 ml of deionized water. A white solid obtained following evaporation of the water was calcined in air at 773 K for 5 h to give a dark blue solid. The calcined solid was subsequently reduced by heating from room temperature to 923 K at a rate of 1 K/min in flowing H_2 (150 ml/min), followed by cooling to room temperature. The sample was then flushed with He (60 ml/min) for 15 min and subsequently passivated in a flow of 1.0 mol% O_2/He (30 ml/min) for 2 h to yield unsupported MoP. The He (Airgas, 99.999%) and H_2 (Airgas, 99.999%) were purified prior to use by passing through 5A molecular sieve (Alltech) and O_2 (Oxyclear) purification traps.

MoP/SiO_2. MoP/SiO_2 catalysts were prepared with theoretical MoP loadings of 15, 25, and 40 wt%. The silica (SiO_2) support (Cab–O–Sil, M-7D grade, 200 m^2/g) was calcined at 773 K for 3 h prior to use. Impregnating solutions were prepared by dissolving enough $(NH_4)_6Mo_7O_{24} \cdot 4H_2O$ and $(NH_4)_2HPO_4$ in water to give the desired loading. Multiple impregnations were necessary to prepare the catalysts with 25 and 40 wt% MoP loadings. The impregnating solution was added dropwise to 5.0 g of calcined silica until incipient wetness. The precursor was dried in a 393-K oven,

0021-9517/02 $35.00

calcined in air at 773 K for 3 h, and then reduced in flowing hydrogen (150 ml/min) with the temperature ramped from room temperature to 923 K (1 K/min). The sample was then cooled to room temperature, flushed with flowing He (60 ml/min) for 15 min, and passivated in a flow of 1.0 mol% O_2/He (30 ml/min) for 2 h to yield silica-supported MoP.

MoO_3/SiO_2. For comparison purposes, a MoO_3/SiO_2 catalyst (16.7 wt% MoO_3, 11.1 wt% Mo) was prepared with a Mo loading similar to that of the 15 wt% MoP/SiO_2 catalyst (11.3 wt% Mo). Calcined silica was impregnated with a solution of $(NH_4)_6Mo_7O_{24} \cdot 4H_2O$ to give the desired metal loading. The resulting precursor was dried in a 393-K oven and calcined in air at 773 K for 3 h.

Catalyst Characterization

X-ray diffraction measurements. X-ray diffraction (XRD) patterns were acquired for the MoP/SiO_2 catalysts on a Rigaku Geigerflex powder diffractometer using the Vaseline® smear method. The system uses Cu $K\alpha$ radiation ($\lambda = 1.5418$ Å) and is interfaced to a personal computer for data acquisition and analysis.

Electron microscopy. Transmission electron microscope (TEM) images were acquired using a JEOL 2010 high-resolution TEM operating at 200 keV. Samples of the MoP/SiO_2 catalysts were placed on a 200-mesh copper grid coated with formvar and carbon.

Scanning electron microscopy (SEM) measurements were carried out using a LEO 982 field emission scanning electron microscope (FESEM) equipped with an Oxford ISIS energy-dispersive microanalysis system. Samples of the MoP/SiO_2 catalysts were carbon-coated using an Edwards S150B Sputter Coater with a carbon evaporation unit.

XPS measurements. X-ray photoelectron spectroscopy (XPS) measurements were carried out using a Physical Electronics Quantum 2000 Scanning ESCA Microprobe system. This system uses a focused monochromatic Al $K\alpha$ X-ray (1486.7 eV) source and a spherical section analyzer. The XPS spectra were collected using a pass energy of 23.5 eV. The spectra were referenced to an energy scale with binding energies for Cu $2p_{3/2}$ at 932.67 ± 0.05 eV and for Au 4f at 84.0 ± 0.05 eV. Low-energy electrons and argon ions were used for specimen neutralization.

BET and pulsed chemisorption measurements. Single-point BET surface area measurements were obtained using a Micromeritics PulseChemisorb 2700 apparatus. Catalyst samples (~0.10 g) were placed in a quartz U-tube, degassed in a 60 ml/min flow of He for 30 min at room temperature followed by a 2-h degassing in a 45 ml/min flow of He at 623 K, then cooled to room temperature under flowing He. The BET measurements were then carried out as described previously (3).

CO and O_2 pulsed chemisorption measurements were also carried out using the Micromeritics PulseChemisorb 2700 instrument. Chemisorption capacity measurements were conducted using CO (Airco, 99.999%) and a 10.3 mol% O_2/He mixture (Airco) as probe gases. All catalyst samples (~0.10 g) were degassed in a 60 ml/min flow of He at room temperature for 30 min and were then either reduced or sulfided prior to the chemisorption measurement. Samples were reduced by heating from room temperature to 673 K (6.3 K/min) in a 60 ml/min flow of H_2 and holding at 673 K for 2 h. Samples were sulfided by heating from room temperature to 650 K (5.9 K/min) in a 60 ml/min flow of 3 mol% H_2S/H_2 and holding at 650 K for 2 h. The sulfided samples were then reduced in a 60 ml/min flow of H_2 at 623 K for 1 h. Finally, all samples were degassed in 45 ml/min He at 673 K for 1 hr. The chemisorption capacity measurements were carried out as described elsewhere (3). The CO and O_2 chemisorption studies were carried out at 273 and 196 K, respectively.

Thiophene HDS Activity Measurements

Thiophene HDS activity measurements were carried out using an atmospheric pressure flow reactor outfitted with a gas chromatograph (HP 5890 Series II). The gas chromatograph is equipped with a flame ionization detector for online analysis of thiophene and hydrocarbon products. The flow reactor system and the specifics of the HDS activity measurements have been described in detail elsewhere (3). The reactor feed in the current study consisted of a 3.2 mol% thiophene/H_2 mixture.

Prior to the measurement of thiophene HDS activities, MoP/SiO_2 catalysts were subjected to one of three different pretreatments: (i) degassing in He (60 ml/min) at room temperature for 30 min, (ii) reduction in H_2 by heating the catalyst sample from room temperature to 673 K (6.3 K/min) in a 60 ml/min flow of H_2 and holding at 673 K for 2 h, and (iii) sulfidation by heating from room temperature to 650 K (5.9 K/min) in a 60 ml/min flow of 3 mol% H_2S/H_2 and holding at 650 K for 2 h. Following pretreatment, the temperature was adjusted to the reaction temperature of 643 K and the flow was switched to the 3.2 mol% thiophene/H_2 reactor feed (50 ml/min). The reaction was carried out for 24–150 h, with automated sampling of the gas effluent occurring at 1-h intervals. Thiophene HDS activities (nmol of Th/g of cat s) were calculated from the total product peak areas calculated from the chromatogram after either 24 or 150 h of reaction time.

RESULTS

Catalyst Characterization

Shown in Fig. 1 are XRD patterns for MoP/SiO_2 catalysts with 15, 25, and 40 wt% MoP loadings as well as for the

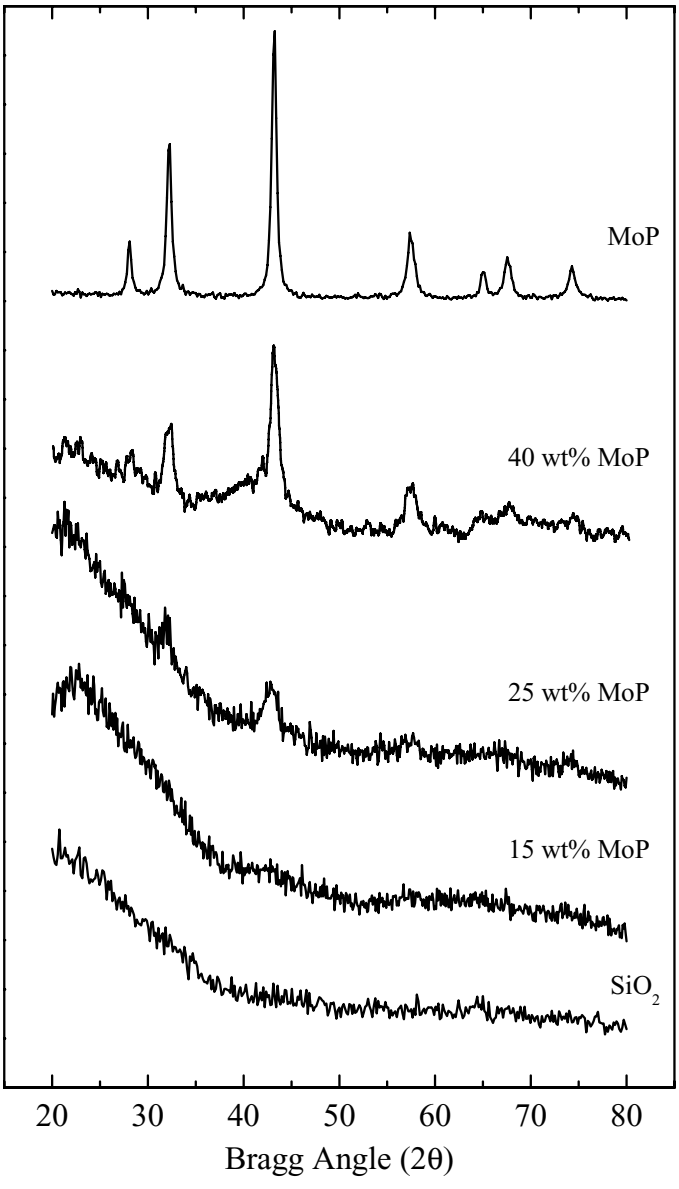

FIG. 1. X-ray diffraction patterns for the silica support, for 15, 25, and 40 wt% MoP/SiO_2 catalysts, and for unsupported MoP.

SiO_2 support and unsupported MoP. The XRD pattern of unsupported MoP shows peaks at 28.0, 32.2, 43.2, 57.3, 64.9, 67.4, and 74.3° and is similar to those reported by others (8–10) as well as to a reference pattern for MoP taken from the JCPDS powder diffraction file (card 24-771) (11). The XRD patterns for the 25 and 40 wt% MoP/SiO_2 catalysts exhibit these same peaks, confirming the presence of MoP on the silica support. Using the Scherrer equation (12) and the full width at half maximum of the {101} reflection at 43.1°, a MoP particle size of ∼5.9 nm can be calculated for the 25 wt% MoP/SiO_2 catalyst. No XRD peaks are apparent in the XRD pattern for the 15 wt% MoP/SiO_2 catalyst other than a broad feature at ∼43°.

Shown in Fig. 2 are TEM images of a 25 wt% MoP/SiO_2 catalyst. Inspection of Fig. 2a indicates the presence of MoP particles of a fairly uniform size dispersed on the silica support. Figure 2b shows a silica-supported MoP particle with a diameter of ∼7.2 nm, which is consistent with the particle size calculation from the XRD pattern for this same catalyst. The TEM image in Fig. 2b yields d-spacing values of 2.12 and 2.79 Å for the {100} and {101} crystallographic planes of MoP, respectively, which are in excellent agreement with those from the JCPDS powder diffraction file for MoP (card 24-0771) (11). SEM energy-dispersive X-ray analysis of a 25 wt% MoP/SiO_2 catalyst yielded an elemental composition of 12.7 atom% Mo and 14.1 atom% P, which is in good agreement with the 1:1 stoichiometry of MoP.

XPS spectra in the Mo 3d and P 2p regions for the calcined MoP precursor of unsupported MoP, for a 25 wt% MoP/SiO_2 catalyst, and for unsupported MoP are shown in Fig. 3. The XPS spectra indicate the presence Mo and P species with one or more oxidation states at the surface of the different materials, but strong similarities are apparent for the spectra of unsupported and silica-supported MoP. Following their synthesis, the unsupported MoP and the MoP/SiO_2 catalysts are passivated in a flow of a 1 mol% O_2/He mixture which forms an oxide layer on the surface of the MoP particles, which protects them from deep oxidation. As a result, it is not surprising that some of the XPS peaks for the unsupported MoP and the 25 wt% MoP/SiO_2 catalyst correspond to highly oxidized Mo and P species. The most intense Mo $3d_{5/2}$ peak for all three materials is located at 232.7–233.8 eV, which lies in the range reported by others for Mo^{6+} species [232.2–233.8 eV (13–18)]. It is not known why the Mo $3d_{5/2}$ peak associated with Mo^{6+} species appears at 233.8 eV for the calcined MoP precursor and the MoP/SiO_2 catalyst, and at 232.7 eV for unsupported MoP. The XPS spectra for the calcined MoP precursor and the MoP/SiO_2 catalyst do show a shoulder at 232.2–232.7 eV that also lies in the binding energy range associated with Mo^{6+} species. The XPS spectra for the unsupported and silica-supported MoP contain a small Mo $3d_{5/2}$ peak at 228.4 eV which lies at a slightly higher binding energy than is assigned to metallic Mo (Mo^0) [227.4–227.8 eV (13, 17, 18)], and at the low end of the range assigned to Mo^{4+} species in MoS_2 [228.3–231.8 eV (13–18)].

The XPS spectra in the P 2p region show a large peak at 133.8–133.9 eV for the calcined MoP precursor, for the 25 wt% MoP/SiO_2 catalyst, and for unsupported MoP as well as a smaller peak at 129.6 eV for the latter two materials. Okamoto *et al.* (19–21) used XPS to investigate the surfaces of amorphous Ni–P catalysts. Consistent with our results for MoP catalysts, the XPS spectra of the Ni–P catalysts showed two kinds of phosphorus species, with P $2p_{3/2}$ binding energies of 129.7 and 134.0 eV, which are shifted in opposite directions from the value for elemental

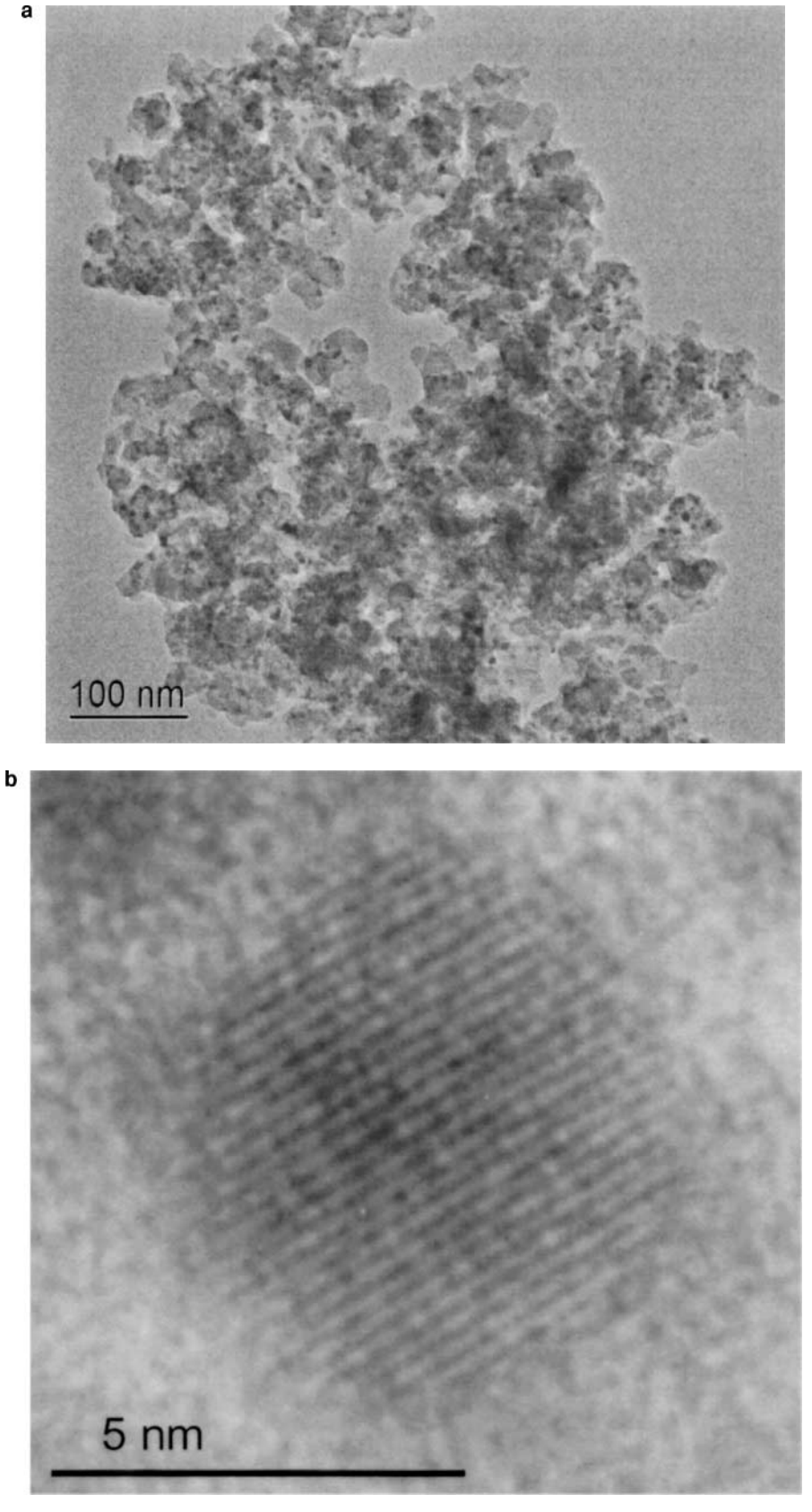

FIG. 2. TEM micrographs of a 25 wt% MoP/SiO_2 catalyst.

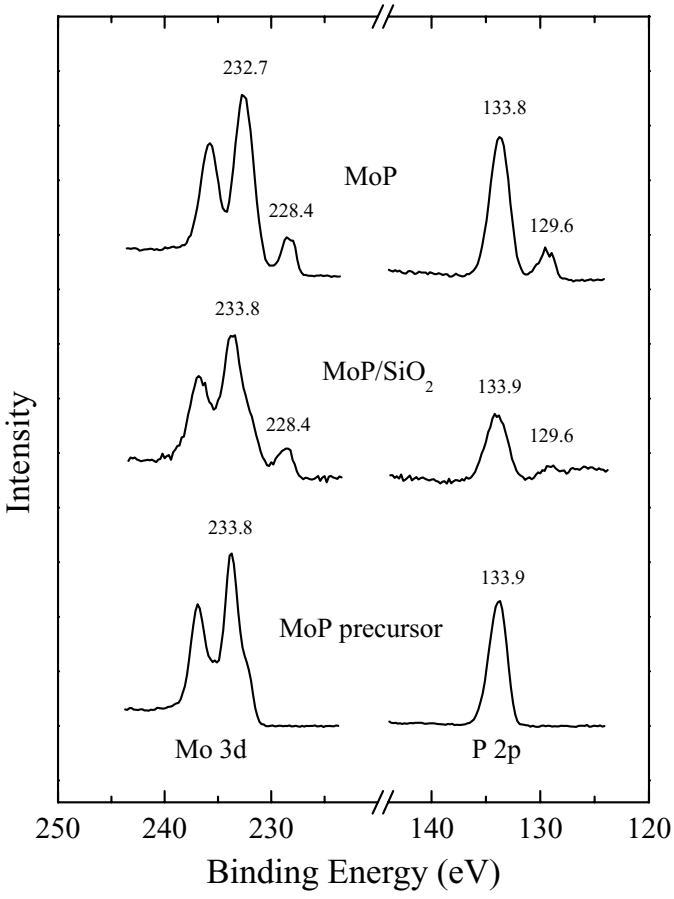

FIG. 3. XPS spectra in the Mo 3d and P 2p regions for an oxidic MoP precursor, a 25 wt% MoP/SiO_2 catalyst, and unsupported MoP.

phosphorus (130.4 eV) (20). Oyama and coworkers (22) reported XPS spectra for an unsupported tungsten phosphide (WP) catalyst and observed peaks in the P 2p region at 130.0 and 134.6 eV. Okamoto *et al.* (19–21) concluded that the phosphorus species with a XPS P $2p_{3/2}$ binding energy of 129.7 eV was associated with P bonded to Ni, while the phosphorus with a binding energy of 134.0 eV was due to surface PO_4^{3-} species. Based upon these assignments, the XPS peaks in the P $2p_{3/2}$ region at 129.6 and 133.9 eV for

TABLE 1

BET Surface Areas and Chemisorption Capacities

Catalyst	Surface area (m^2/g)	Chemisorption capacities (μmol/g)			
		CO		O_2	
		Reduced	Sulfided	Reduced	Sulfided
Sulf. Mo/SiO_2[a]	110	—	15.0	—	10.2
15 wt% MoP/SiO_2	89	103.2	56.0	138.2	44.8

[a] This catalyst has a Mo loading similar to that of the 15 wt% MoP/SiO_2 catalyst.

TABLE 2

Thiophene HDS Activities after 150 h on-Stream

Catalyst	HDS activity (nmol of Th/g of cat/s)	Relative HDS activity
Sulfided Mo/SiO_2[a]	245	1.00
15 wt% MoP/SiO_2	898	3.66
25 wt% MoP/SiO_2	1032	4.21

[a] This catalyst has a Mo loading similar to that of the 15 wt% MoP/SiO_2 catalyst.

unsupported and silica-supported MoP are assigned to P bonded to Mo (i.e., phosphide) and to PO_4^{3-} species.

The BET surface areas as well as CO and O_2 chemisorption capacities for the 15 wt% MoP/SiO_2 and sulfided Mo/SiO_2 catalysts are listed in Table 1. For the MoP/SiO_2 catalysts, chemisorption measurements were carried out on both sulfided and reduced catalyst samples. The MoP/SiO_2 catalysts have higher chemisorption capacities than do the sulfided Mo/SiO_2 catalysts. A sulfidation pretreatment substantially lowers the chemisorption capacities of the MoP/SiO_2 catalysts relative to the same catalysts subjected to a reduction pretreatment.

Catalyst Evaluation

Thiophene HDS activities as a function of time on-stream for 15 and 25 wt% MoP/SiO_2 catalysts as well as for a sulfided Mo/SiO_2 catalyst with a metal loading similar to the 15 wt% MoP/SiO_2 catalyst are shown in Fig. 4, and the HDS activities after 150 h are given in Table 2. The MoP/SiO_2 catalysts were pretreated only by degassing in flowing He prior to being brought on-stream. The MoP/SiO_2 catalysts

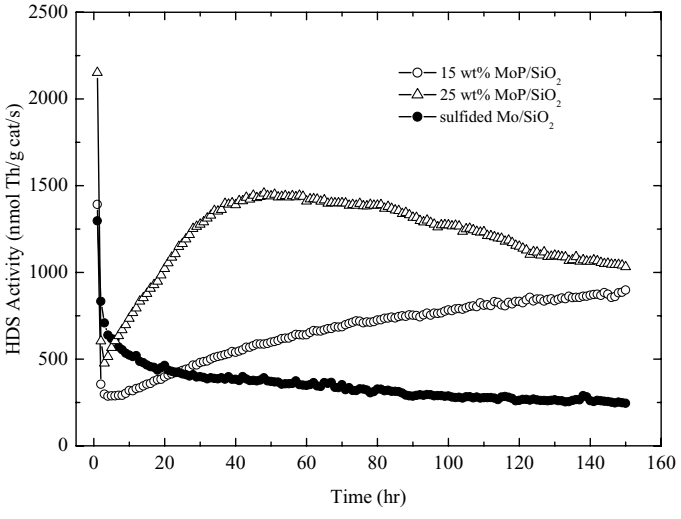

FIG. 4. Thiophene HDS activity data for 15 and 25 wt% MoP/SiO_2 catalysts, as well as for a sulfided Mo/SiO_2 catalyst with a Mo loading similar to that of the 15 wt% MoP/SiO_2 catalyst.

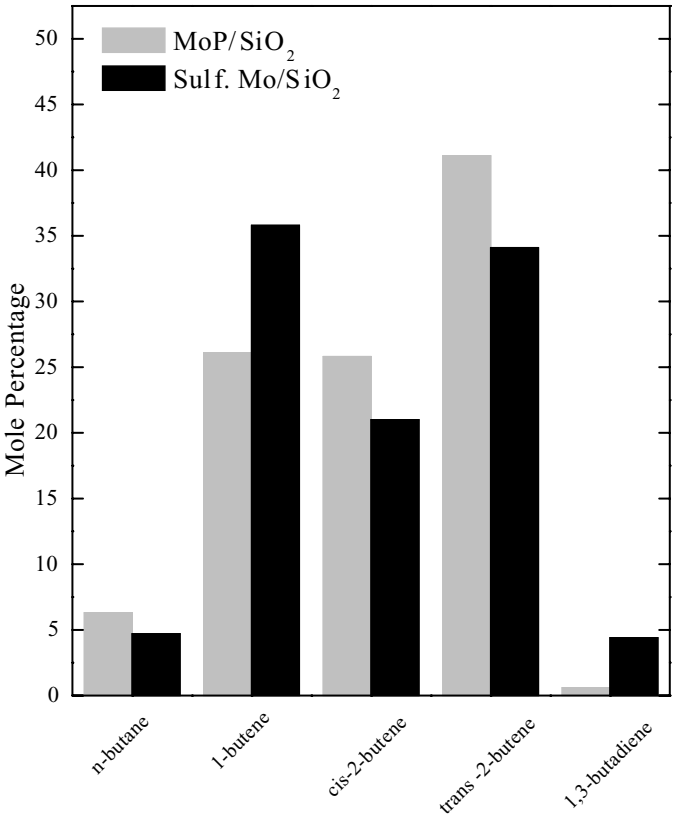

FIG. 5. Thiophene HDS product distributions after 150 h for a 15 wt% MoP/SiO_2 catalyst and a sulfided Mo/SiO_2 catalyst with a similar Mo loading.

exhibit an unusual trend in which their HDS activities increase substantially over time following an initial decline after the catalysts are brought on-stream. An increase in HDS activity is observed for the first 50 h for the 25 wt% MoP/SiO_2 catalyst, and for the entire 150-h time period for the 15 wt% MoP/SiO_2 catalyst. After 150 h, the 15 wt% MoP/SiO_2 catalyst is nearly four times more active than a sulfided Mo/SiO_2 catalyst with a similar Mo loading. Shown in Fig. 5 are the thiophene HDS product distributions for the 15 wt% MoP/SiO_2 catalyst and the sulfided Mo/SiO_2 catalyst, both after 150 h on-stream. Thiophene HDS over the MoP/SiO_2 catalyst produces more *cis*- and *trans*-2-butene, and less 1-butene and 1,3-butadiene relative to the sulfided Mo/SiO_2 catalyst. Butene isomer ratios calculated from the product distribution for the MoP/SiO_2 catalyst, *cis*-2-butene/*trans*-2-butene = 0.70 and 1-butene/2-butene = 0.39, are consistent with those predicted for thermodynamic equilibrium of the isomers, *cis*-2-butene/*trans*-2-butene = 0.70 and 1-butene/2-butene = 0.34 (23).

Thiophene HDS activity measurements were also carried out for 15 wt% MoP/SiO_2 catalysts that were subjected to the three different pretreatments (He degassing, reduction in H_2, and sulfidation in H_2S/H_2) described under Experimental Methods. These HDS activity measurements were carried out for 24 h and the HDS activities of the MoP/SiO_2 catalysts were observed to be sensitive to the pretreatment used. The relative HDS activities of the differently pretreated MoP/SiO_2 catalysts increased in the order sulfidation (1.00) < reduction (1.44) < He degassing (1.62). In each case, the MoP/SiO_2 catalysts exhibited an increasing trend of HDS activity similar to that shown in the initial 24 h of the data plotted in Fig. 4.

DISCUSSION

Phosphorus is added to commercial hydrotreating catalysts used for the hydrodenitrogenation (HDN) of heavy feedstocks (1) and a number of studies have addressed the effect of added phosphorus on the hydrotreating properties of Mo-based catalysts, as has been recently reviewed (24). Possible effects for added phosphorus include increased mechanical and thermal stability of the alumina support due to the formation of $AlPO_4$, decreased interaction between molybdate species and the support which leads to the formation of MoS_2-like structures with different particle morphologies, and increased catalyst acidity (1). Focusing on studies in which the effects of added phosphorus on HDS properties were addressed, phosphorus has been observed to have no effect or to increase the HDS activity of sulfided Mo/Al_2O_3 catalysts (24). Fierro *et al.* (25) as well as Lewis and Kydd (26) found the addition of phosphorus to increase the thiophene HDS activity of sulfided Mo/Al_2O_3 catalysts by as much as a factor of two. The positive effects of added phosphorus on HDS activity were traced to molybdena species being more easily sulfided (26) and to changes in the morphology of supported MoS_2 slabs (25).

Only recently has attention been focused on the hydrotreating properties of MoP (8–10). Based upon *o*-propylaniline HDN activity measurements, Prins and coworkers (9) estimated unsupported MoP to have an intrinsic HDN activity about six times higher than that of a sulfided Mo/Al_2O_3 catalyst. Oyama and coworkers (10) found MoP/Al_2O_3 catalysts to be more than twice as active for HDN and of slightly higher activity for HDS of a model petroleum feed compared to a sulfided Ni–Mo/Al_2O_3 catalyst.

The fact that only a small number of studies have been published concerning the catalytic properties of MoP, both unsupported and supported, has been in part due to the difficulty and inconvenience of preparing this material in high-surface-area form. Muetterties and Sauer (27) prepared MoP/Al_2O_3 catalysts by treating alumina-supported $Mo(CO)_6$ with phosphine (PH_3) for 3 h at 573 K. However, the high toxicity of PH_3 greatly limits the usefulness of this synthesis method. More recently, Oyama and coworkers (8, 10) have reported a synthesis procedure for preparing unsupported and alumina-supported MoP that involves the

reduction of a phosphate-like precursor ($MoPO_{5.5}$) in H_2. This synthesis procedure does not utilize PH_3 and allows preparation of MoP dispersed on a high-surface-area oxide support.

The synthesis procedure employed in the current study for the preparation of MoP/SiO_2 catalysts is similar in most details to that reported by Oyama and coworkers (10) for MoP/Al_2O_3 catalysts, but differs in that the maximum temperature reached in the temperature-programmed reduction was 923 K for the MoP/SiO_2 catalysts versus 1123 K for the MoP/Al_2O_3 catalysts. This difference in the reduction temperature needed to convert the supported phosphate precursor to MoP is most likely due to the greater difficulty in reducing Mo species on alumina than on silica (14, 28, 29).

As described under Results, the XRD patterns in Fig. 1 and TEM images in Fig. 2 for a 25 wt% MoP/SiO_2 catalyst confirm the successful synthesis of silica-supported MoP. The presence of only a very weak and broad peak at $\sim 43^\circ$ in the XRD pattern of a 15 wt% MoP/SiO_2 catalyst (Fig. 1) does not allow direct identification of a Mo phase on the silica support. Instead, the synthesis of MoP on the support is inferred for this catalyst, with the assumption that the MoP particle size is below the XRD detection limit. The substantial CO and O_2 chemisorption capacities for 15 wt% MoP/SiO_2 catalysts (Table 2) subjected to reduction and sulfidation pretreatments are consistent with a high dispersion of MoP on the silica support. The CO and O_2 chemisorption capacities of the 15 wt% MoP/SiO_2 catalyst, whether reduced or sulfided, are substantially higher than those of a sulfided Mo/SiO_2 catalyst with a similar Mo loading. This is not surprising, as it is expected that all surface planes of MoP can adsorb CO or O_2, while only edge planes of MoS_2 adsorb these same gases.

The XPS spectra in the Mo 3d and P 2p regions (Fig. 3) are quite similar for unsupported MoP and a 25 wt% MoP/SiO_2 catalyst, showing the presence of at least two kinds of Mo and P species. The predominant Mo and P species at the catalyst surface have Mo $3d_{5/2}$ and P $2p_{3/2}$ binding energies of 232.7–233.8 and 133.8–133.9 eV, respectively, which are assigned to Mo^{6+} and P^{5+} states, produced during the controlled passivation of the materials in a 1 mol% O_2/He mixture following their synthesis. While it is assumed that the Mo^{6+} and P^{5+} species are in the passivation layer on the surfaces of the MoP particles, it is possible that their presence is instead associated with incomplete reduction of the calcined precursors to MoP. In addition to the XPS peaks associated with oxidized Mo and P species, smaller peaks are observed in the Mo 3d and P 2p regions of the XPS spectra of unsupported MoP and the 25 wt% MoP/SiO_2 catalyst at 228.4 and 129.6 eV, respectively. As described under Results, this P $2p_{3/2}$ peak is assigned to P bonded to Mo (i.e., phosphide) and is shifted to a lower binding energy than for elemental phosphorus [130.4 eV (20)]. The binding energy of 228.4 eV for the Mo species is more difficult to assign, but corresponds to a $Mo^{\delta+}$ species ($0 < \delta \leq 4$). These assignments are consistent with a transfer of electron density from Mo to P in unsupported and silica-supported MoP.

The thiophene HDS activity data reported in this study for MoP/SiO_2 catalysts suggest that oxide-supported MoP is a promising material for use in industrial HDS catalysts. The 15 wt% MoP/SiO_2 catalyst is nearly four times more active (on a per gram of catalyst basis) than a sulfided Mo/SiO_2 catalyst with a nearly identical Mo loading after the catalysts have been on-stream in an HDS reactor for 150 h. Interestingly, excluding a decline during the first 3 h of measurement, the HDS activity of the 15 wt% MoP/SiO_2 catalyst was observed to increase monotonically and had not yet achieved a steady state value after 150 h. The 25 wt% MoP/SiO_2 catalyst also showed an increase in HDS activity after the catalyst was brought on-stream, but in this case only for the first 50 h. After 150 h, the 25 wt% MoP/SiO_2 catalyst is over four times more active (on a per gram of catalyst basis) than the sulfided Mo/SiO_2 catalyst. The observed trends in HDS activity for the MoP/SiO_2 catalysts are in contrast to that of the sulfided Mo/SiO_2 catalyst, which exhibited a steadily decreasing thiophene HDS activity over the entire 150-h measurement. The catalytic behavior of the MoP/SiO_2 catalysts is quite unusual. Thiophene HDS activity measurements in our laboratory for alumina-supported Mo_2C, MoC_{1-x} ($x \approx 0.5$), and Mo_2N catalysts (3, 4), as well as for alumina-supported Cu, Mo, and Rh sulfide catalysts (3, 4, 30), have shown similar behavior to the sulfided Mo/SiO_2 catalyst in the current study, with catalyst activity either decreasing during the entire HDS reaction or achieving steady state activity only after decreasing for the first 16–24 h on-stream. The trend in HDS activity observed for the 15 wt% MoP/SiO_2 catalyst indicates that the surface of the MoP particles evolves into a more active structure over the course of the 150-h activity measurement. Similar behavior was observed for He degassing, H_2 reduction, and sulfidation pretreatments; in each case the HDS activity of the MoP/SiO_2 catalysts was observed to increase after an initial decline. A sulfidation pretreatment had a detrimental effect on the HDS activity of the MoP/SiO_2 catalyst, suggesting that incorporation of sulfur into the surface of the catalyst is not responsible for the increasing HDS activity. Given the unusual catalytic behavior of the MoP/SiO_2 catalysts, it is not obvious what an appropriate method is for normalizing its HDS activity, as the chemisorption capacities of neither the reduced nor the sulfided MoP/SiO_2 catalyst appear to accurately reflect the active catalytic surface under HDS conditions. This contrasts with earlier work in our laboratory in which Mo_2C/Al_2O_3 and Mo_2N/Al_2O_3 catalysts were shown to become sulfided under HDS reaction conditions and the chemisorption capacities of *sulfided* Mo_2C/Al_2O_3 and Mo_2N/Al_2O_3 catalysts provided an excellent estimate of the active site densities (3, 4).

The HDS activities reported for MoP/SiO_2 and sulfided Mo/SiO_2 catalysts in Table 2 are normalized on the basis of catalyst mass. Since the Mo loadings are nearly identical for the 15 wt% MoP/SiO_2 catalyst (11.3 wt% Mo) and the sulfided Mo/SiO_2 catalyst (11.1 wt% Mo), the HDS activities normalized per mole of molybdenum are similar to those normalized on a mass basis, with the MoP/SiO_2 catalyst 3.5 times more active than the sulfided Mo/SiO_2 catalyst. Studies are currently under way in our laboratory to determine the structure and composition of the active catalytic surface of MoP/SiO_2 catalysts under HDS reaction conditions and to develop a suitable measure of the active site density.

ACKNOWLEDGMENTS

This research was supported by the National Science Foundation under Grant CHE-0101690. Acknowledgment is also made to the Henry Dreyfus Teacher–Scholar Awards Program of the Camille and Henry Dreyfus Foundation for partial support of this research. One of us (DCP) acknowledges the Materials Research Society Undergraduate Materials Research Initiative (UMRI) Program for support of this research. A portion (XPS, SEM, TEM) of the research described in this paper was performed in the Environmental Molecular Sciences Laboratory, a national scientific user facility sponsored by the Departments of Energy's Office of Biological and Environmental Research and located at Pacific Northwest National Laboratory. The authors acknowledge Dr. C. H. F. Peden for helpful discussions.

REFERENCES

1. Kabe, T., Ishihara, A., and Qian, W., "Hydrodesulfurization and Hydrodenitrogenation: Chemistry and Engineering." Wiley–VCH, Weinheim, 1999.
2. Sajkowski, D. J., and Oyama, S. T., *Appl. Catal. A* **134**, 339 (1996).
3. Aegerter, P. A., Quigley, W. W. C., Simpson, G. J., Ziegler, D. D., Logan, J. W., McCrea, K. R., Glazier, S., and Bussell, M. E., *J. Catal.* **164**, 109 (1996).
4. McCrea, K. R., Logan, J. W., Tarbuck, T. L., Heiser, J. L., and Bussell, M. E., *J. Catal.* **171**, 255 (1997).
5. Nagai, M., Miyao, T., and Tuboi, T., *Catal. Lett.* **18**, 9 (1993).
6. Nagai, M., Uchino, O., Kusgaya, T., and Omi, S., *in* "Hydrotreatment and Hydrocracking of Oil Fractions" (G. Froment, B. Delmon, and P. Grange, Eds.), p. 541. Elsevier, New York, 1997.
7. Nagai, M., Kiyoshi, M., Tominaga, H., and Omi, S., *Chem. Lett.* 702 (2000).
8. Li, W., Dhandapani, B., and Oyama, S. T., *Chem. Lett.* 207 (1998).
9. Stinner, C., Prins, R., and Weber, T., *J. Catal.* **191**, 1 (2000).
10. Oyama, S. T., Clark, P., Teixiera da Silva, V. L. S., Lede, E. J., and Requejo, F. G., *J. Phys. Chem. B* **105**, 4961 (2001).
11. *JCPDS Powder Diffraction File*, International Centre for Diffraction Data, Swarthmore, PA, 2000.
12. Suryanarayana, C., and Norton, M. G., "X-ray Diffraction: A Practical Approach." Plenum, New York, 1998.
13. Zingg, D. S., Makovsky, L. E., Tischer, R. E., Brown, F. R., and Hercules, D. M., *J. Phys. Chem.* **84**, 2898 (1980).
14. Muralidhar, G., Concha, B. E., Bartholomew, G. L., and Bartholomew, C. H., *J. Catal.* **89**, 274 (1984).
15. Grunert, W., Stakheev, A. Y., Feldhaus, R., Anders, K., Shpiro, E. S., and Minachev, K. M., *J. Phys. Chem.* **95**, 1323 (1991).
16. de Yong, A. M., Borg, H. J., van Ijzendoorn, L. J., Soundant, W. G. F. M., de Beer, V. H. J., van Veen, J. A. R., and Niemantsverdriet, J. W., *J. Phys. Chem.* **97**, 6477 (1993).
17. Spevack, P. A., and McIntyre, N. S., *J. Phys. Chem.* **97**, 11020 (1993).
18. Spevack, P. A., and McIntyre, N. S., *J. Phys. Chem.* **97**, 11031 (1993).
19. Okamoto, Y., Nitta, Y., Imanaka, T., and Teranishi, S., *J. Catal.* **64**, 397 (1980).
20. Okamoto, Y., Nitta, Y., Imanaka, T., and Teranishi, S., *J. Chem. Soc. Faraday Trans.* **75**, 2027 (1980).
21. Okamoto, Y., Fukino, K., Imanaka, T., and Teranishi, S., *J. Catal.* **74**, 173 (1982).
22. Clark, P., Li, W., and Oyama, S. T., *J. Catal.* **200**, 140 (2001).
23. Benson, S. W., and Base, A. W., *J. Am. Chem. Soc.* **85**, 1385 (1963).
24. Iwamoto, R., and Grimblot, J., *Adv. Catal.* **44**, 417 (1999).
25. Fierro, J. L. G., Agudo, A. L., Esquivel, N., and Cordero, R. L., *Appl. Catal.* **48**, 353 (1989).
26. Lewis, J. M., and Kydd, R. A., *J. Catal.* **136**, 478 (1992).
27. Muetterties, E. L., and Sauer, J. C., *J. Am. Chem. Soc.* **96**, 3410 (1974).
28. Peri, J. B., *J. Phys. Chem.* **86**, 1615 (1982).
29. Verbruggen, N. F. D., and Knozinger, H., *Langmuir* **10**, 3148 (1994).
30. Mills, P., Phillips, D. C., Woodruff, B. P., Main, R., and Bussell, M. E., *J. Phys. Chem. B* **104**, 3237 (2000).